NASA Technical Memorandum 58224

NASA-TM-58224 19800017497

A Diffusion Climatology for Cape Canaveral, Florida

Richard K. Siler

April 1980

National Aeronautics and
Space Administration

Lyndon B. Johnson Space Center
Houston, Texas 77058

NASA Technical Memorandum 58224

A Diffusion Climatology for Cape Canaveral, Florida

Richard K. Siler
Lyndon B. Johnson Space Center
Houston, Texas

National Aeronautics and Space Administration

Scientific and Technical Information Office

1980

CONTENTS

TABLES

FIGURES

SUMMARY

Because the effluent from the exhaust cloud produced by a Space Shuttle launch will pose a potential hazard to plant and animal life in the Cape Canaveral area, studies were undertaken to enable launch personnel to make predictions concerning the dispersal of such a cloud as a consideration for launch. To this end, nine basic weather patterns were identified and evaluated as to the probability of occurrence, the probability of onshore/alongshore cloud transport, and the probability of precipitation accompanying the latter. In addition, hydrogen chloride diffusion estimates for 79 case days were tabulated, based on concentration calculations, including the distance from the launch site to where the concentrations occurred, and the percentage of clouds that moved onshore. The results of this study showed that synoptic meteorology is a much stronger determinant of the weather regime than are diurnal variations. Likewise, onshore cloud transport, with or without precipitation, is apparently unaffected by time of day.

Idealized weather maps showing the basic synoptic weather regimes and cloud transport probability maps for the Cape Canaveral area were constructed for each weather pattern to help in classifying prognostic charts and determining the most probable groundpath of the launch cloud.

INTRODUCTION

The launch of a Space Shuttle will produce a large, toxic cloud formed by the exhaust products that will rise from the surface to a stabilization height of 1 to 1.5 kilometers within a few minutes. There, the cloud will move with the prevailing winds and will expand both vertically and horizontally. Depending on meteorological conditions, the exhaust products may reach the Earth in relatively high concentrations, not at all, or, more usually, in some quantity between the two extremes.

Two important problems have thus arisen: (1) the prediction of ground-level concentrations of hydrogen chloride (HCl) and (2) the prediction of the groundpath of the cloud. To expose any population or food crop to dangerous or damaging concentrations of toxic materials would be undesirable. Conversely, it is also important that Space Shuttle launches not be delayed unnecessarily. The NASA Marshall Space Flight Center Multilayer Diffusion Model (MDM) was developed to solve these problems and for certain cases it is effective (ref. 1). However, diffusion estimates are more accurate when the weather input data are measured as near to launch time as possible. Diffusion estimates 1 or 2 days before launch would never cause a launch to be rescheduled, but they will be a part of

the total information package available to the launch team to aid in making their launch-operation decisions.

To gain more insight into this long-range prediction problem, a more general, probabilistic approach is presented. This approach uses standard National Oceanic and Atmospheric Administration (NOAA) National Weather Service products and a specially developed diffusion climatology. The climatology and techniques developed in this study can be objectively applied by the operational meteorologist.

In compliance with NASA's publication policy, the original units of measure have been converted to the equivalent value in the Système International d'Unités (SI). As an aid to the reader, the SI units are written first and the original units are written parenthetically thereafter.

BACKGROUND

In response to legal requirements set forth in the National Environmental Policy Act of 1969, NASA established the Environmental Effects Project Office (EEPO) with the task of investigating the impact of Space Shuttle operations on the environment and of publishing the findings in an Environmental Impact Statement. The EEPO was established in 1974, within the Shuttle Program Office. Management responsibility was assigned to the NASA Lyndon B. Johnson Space Center (JSC), with NASA Langley Research Center (LaRC), NASA George C. Marshall Space Flight Center (MSFC), and NASA John F. Kennedy Space Center (KSC) contributing expertise to the project.

Of immediate concern was the large quantity of HCl gas that would be released with the burning of the solid rocket booster engines. Gaseous HCl can be hazardous to plant and animal life and hydrochloric acid, which would be formed in "rainout" or "washout" conditions, can also damage vegetation. To assess this problem, the MDM was developed to provide estimates of ground-level concentrations of the several species of exhaust-cloud constituents for those Space Shuttle vehicles launched from Cape Canaveral, Florida. Predicted concentrations of HCl were compared with ground-level measurements of HCl made during several Titan III-C launches (refs. 2 to 4) and, although there are uncertainties with such comparisons, the model appears to predict substantially higher concentrations than those measured.

As a result of the legal requirements to analyze environmental impacts under the Clean Air Act, various diffusion models designed to assess air quality concerns are in wide use. However, all diffusion models are subject to uncertainties. The degree of uncertainty depends on the nature of the release (continuous, elevated, point-source release; continuous, ground-level, area-source release; instantaneous, point-source, ground-level release; etc.); on the amount of released pollutant; on the terrain over which the pollutant travels; on meteorological measurements; and on travel time/distance, among other considerations.

It should be remembered that under the best of circumstances, accuracy within a factor of 2 is a realistic estimate for routine applications. However, buoyant fluid flows, dispersion in extremely stable or unstable atmospheric conditions, and dispersion at downwind distances of 10 to 20 kilometers or more will cause estimates to be less accurate (ref. 5).

APPROACH

The prediction of concentrations and the prediction of cloud movement are meteorological problems. The diffusivity of the atmosphere is a function of turbulent mixing, whereas cloud transport basically depends on wind at the cloud level. If similar weather conditions are grouped, it may be assumed that the cloud will be transported along similar ground-paths and, depending on the time of day, that concentrations will also have similar magnitudes. There will also be a range of meteorological conditions within each group resulting in a range of observed concentrations and cloud movements.

For this study, the weather regimes that dominate the launch area at Cape Canaveral were defined and identified using the surface weather analysis as performed by the National Weather Service in Suitland, Maryland. Such an analysis has a strong relationship to the pattern found in the planetary boundary layer and several kilometers above it. Windspeed and direction at the approximate cloud-stabilization height were tabulated for each case day. Some weather patterns are highly correlated with precipitation and, because "washout" of HCl is important, the occurrence of precipitation for each case was included. So that diurnal effects might be identified, data were tabulated at 00:00, 06:00, 12:00, and 18:00 Greenwich mean time (G.m.t.) each day, except that upper air winds were normally measured only at 00:00 and 12:00 G.m.t.

Using 1965 KSC weather data supplied by MSFC and mixing heights computed by the NOAA Environmental Data and Information Service (EDIS), diffusion estimates were made at JSC for 79 case days, using the NASA MSFC MDM models 3 and 4 programed for use on a PDP 11/45 computer. This approach provides the following information.

1. The identification and frequency of occurrence of the dominant weather regimes in the Cape Canaveral area by time of day and by month

2. The frequency of occurrence of onshore and offshore cloud movement associated with each pattern and also the mean and the standard deviation of windspeed and wind direction near the cloud level

3. The frequency of occurrence of precipitation with onshore cloud transport for each weather regime

4. A statistical summary of maximum surface concentrations of HCl analyzed to show the diurnal effect for each pattern

WEATHER PATTERNS

Weather in the Cape Canaveral area is largely dependent on the strength and position of the subtropical anticyclone and its associated east-west ridge of high pressure. If the ridge lies to the south of the launch area, Cape Canaveral is exposed to weather disturbances in the westerlies (e.g., fronts, or high- and low-pressure areas in the Gulf of Mexico and in the Eastern United States). If the ridge lies to the north, the launch area is susceptible to weather embedded in the easterlies, which generally implies warm air with long overwater trajectories.

From this concept, nine basic weather patterns, or regimes, which make up more than 98 percent of Florida weather patterns, were identified: A1 - subtropical ridge lying to the north of Cape Canaveral (fig. 1), A2 - subtropical ridge lying very close to Cape Canaveral (fig. 2), A3 - subtropical ridge lying to the south of Cape Canaveral (fig. 3), D1 - cold front approaching from the north or northwest (fig. 4), D2 - cold front over southern Florida (fig. 5), B - high pressure centered over the eastern third of the United States (fig. 6), GH - high pressure in the Gulf of Mexico (fig. 7), E - low pressure in the Gulf of Mexico (fig. 8), and LV - weak pressure gradient within 278 kilometers (150 nautical miles) of the launch site (fig. 9). In figures 1 to 9, ddd is the mean wind direction in degrees azimuth at cloud height for all months, V is the mean windspeed in knots at cloud height for all months, S_d is the standard deviation of ddd for all months, P is the probability of pattern occurrence, P_1 is the probability of onshore/alongshore cloud transport, and P_2 is the probability of precipitation and onshore/alongshore cloud transport.

Surface and upper air charts for the years 1968 through 1974 were obtained on loan from the NOAA EDIS library in Silver Spring, Maryland. Measurements of upper winds to 3 kilometers, based on 00:00 and 12:00 G.m.t. soundings, and hourly rainfall amounts measured at Melbourne, Florida, were obtained from the EDIS located in Asheville, North Carolina. The weather maps, valid at 00:00, 06:00, 12:00, and 18:00 G.m.t., were classified according to the preceding criteria. Hourly precipitation amounts were totaled for the 6 hours both preceding and including map time, and upper winds at 1500 meters were tabulated for the 00:00 and 12:00 G.m.t. patterns. This information was analyzed in three ways.

1. For the probability of occurrence of pattern type by time of day, by month, and by year

2. For the probability of onshore/alongshore cloud transport with each weather regime by time of day, by month, and by year

3. For the probability of onshore/alongshore cloud transport occurring with precipitation for each weather type by time of day, by month, and by year

Onshore/alongshore cloud transport is considered to occur when the wind direction at 1500 meters is from 180° through 090° to 320° azimuth. The average orientation of the Florida coastline in the launch-site area is about 160° to 340° azimuth. The 20° difference on either side of this bearing allows for the variability of wind direction with time and space and probably results in a conservative bias in the onshore statistics.

RESULTS

This study provides the meteorologist with a statistical tool whereby he can issue a probability statement regarding launch-cloud transport 24 to 48 hours preceding launch. Some important factors were found as a result of this study. For example, the frequency of pattern occurrence does not vary significantly with time of day; i.e., synoptic meteorology is a much stronger determinant of the weather regime than are diurnal variations. Considering the frequency of occurrence at synoptic mapping times, the greatest difference is 2.2 percent. As might be expected, this difference occurs with the LV pattern when, at 06:00 G.m.t., LV patterns occur with a frequency of 12.6 percent; whereas, at 18:00 G.m.t., that frequency is 10.4 percent. Considering all meteorological uncertainties, this is probably not a significant difference. Similarly, onshore cloud transport, either with or without precipitation, seems to be unaffected by time of day. These statistical data are given in the appendix.

The statistical results of this study are shown in the following tables.

Table I shows the probability of occurrence by month for each pattern. Pattern A1 occurs more than 20 percent of the time and patterns A1, A2, and B have a combined frequency of occurrence of almost 50 percent. Seasonal variation exists strongly for each pattern except for pattern E.

Table II shows the probability of onshore/alongshore cloud transport, given the existing weather regime. Some patterns strongly favor onshore winds whereas others will usually produce offshore winds. A seasonal preference is also shown in these data. The A2 and LV February anomalies defy explanation, but most other variations can be satisfactorily explained. For instance, even though frontal passages are rare summertime events, the probability is high that a front will become stationary and that onshore winds will occur. The relatively high frequency of onshore winds associated with pattern E from June through October reflects the influence of tropical-storm activity during those months.

Table III shows the probability of precipitation occurring with onshore/alongshore cloud transport.

In considering tables I to III, pattern A1 would occur $365 \times 0.205 = 75$ days per year; the exhaust cloud would move ashore $365 \times 0.205 \times 0.913 = 68$ times; and, of those 68 occurrences, precipitation would occur in the

area 365 × 0.205 × 0.913 × 0.090 = 6 times, or during 6 potential launch days per year.

Table IV is a summary of the diffusion estimates for the 79 case days, where χ is the average peak concentration of HCl in parts per million (p/m), χ_M is the largest concentration calculated from each sample, P_1 is the percent of clouds that moved onshore, and D is the distance in meters from the launch site at which χ occurred. The value P_1 is not listed for model 3 calculations because the computed height of the launch cloud was sometimes as low as 100 meters and, generally, the cloud rise seemed unreliable. Concerning table IV, a cautionary note is necessary. As previously stated, such calculations are subject to uncertainties and it is somewhat misleading to carry these calculations to three decimal places. A more reasonable approach might be to round the computed peak concentrations to the nearest 1 p/m to avoid the error of attaching significance to trivial differences.

Table IV shows that, regardless of weather regime, time of day, or diffusion model used, the average ground-level peak concentration of HCl is approximately 1 p/m. In the largest concentrations, the χ_M averages approximately 2 p/m, although patterns D1 and GH had absolute peak concentrations of nearly 3 p/m. A reasonable conclusion is that peak concentrations associated with these patterns might sometimes exceed the maximum allowable short-term exposure limit of 8 p/m, especially when the minimum uncertainty factor of 2 is considered. Notably, however, all tested cases of D1 clouds moved offshore as did a high percentage of GH clouds. Also of importance is the fact that peak concentrations generally occur within about 6000 meters of the launch site.

The pertinent statistical data found in tables I to IV are shown with corresponding weather patterns. Figures 1 to 9 depict the weather regimes that most commonly affect launch-site weather.

The shaded areas in figures 1(b) to 9(b) show where the launch-exhaust cloud will go approximately 90 percent of the time for each weather pattern. The central vector indicates the mean direction of cloud movement; the bounding vectors were determined by assuming a normal distribution of wind directions; and the concentric arcs represent 1-, 2-, and 3-hour cloud-travel times based on the observed windspeeds at cloud height.

Identification of weather regimes from a weather map can sometimes be difficult because the patterns are never exactly alike. However, as with fingerprints, weather patterns may be grouped according to their dominant characteristics. Within each group, these characteristics will vary between whatever limits have been imposed by the classification criteria, but the real difficulty in pattern identification occurs as the limits are approached. The following discussion will be helpful in making borderline decisions when classifying prognostic charts.

Figure 1, Pattern A1

When the curvature of the east-west ridge of the Bermuda High is strong, the position of that ridge with respect to Cape Canaveral can easily be determined. In this example, the highest surface pressure lies north of the latitude of the launch area, but sometimes the ridge is not so sharply defined. When the curvature is greater, it becomes difficult to distinguish between A1 and A2. A current surface analysis would show the exact surface-pressure distribution, but a prognostic chart would not. Therefore, the history of the ridge should be considered and these questions asked. Has the ridge been moving southward? Does the next prognostic chart suggest the answer? Perhaps an examination of the forecast boundary layer winds will prove helpful. If the forecast winds tend to veer from the southeast to a more southerly direction, then the prognostic chart should be classified A2. If the veering is not evident, A1 is probably the better classification.

Figure 2, Pattern A2

Usually it is difficult to place the ridge closer than approximately 1° latitude, particularly when the curvature of the ridge is great. In these cases, classify the pattern as A2 if the ridge appears to be within 1° latitude of Cape Canaveral. If the boundary layer wind forecast shows no definite trend toward the southeast, classify the pattern as A1, or toward the southwest, as A3. Figure 2 shows the clear-cut A2 pattern with the ridge passing through, or very close to, the launch site.

Figure 3, Pattern A3

Figure 3 represents an idealized example of the A3 pattern, but it is also typical of a case that is becoming borderline. In the cool season, the A3 pattern is frequently followed by a cold front from the northwest. In making this classification, the first thing to be decided in this case, as in all cases, is what synoptic feature is the dominant influence on the surface-wind direction at the launch site. In this example, the Cape Canaveral area is still under the influence of the subtropical ridge; therefore, the classification is A3.

Figure 4, Pattern D1

Whenever the launch-site surface winds are under the direct influence of (i.e., within the circulation of) an approaching cold front, classify the pattern as D1.

Figure 5, Pattern D2

This pattern is usually obvious, but, occasionally, fronts will stall and become stationary in southern Florida. In these cases, the surface-

pressure field may resemble type B with high pressure centered over the eastern third of the United States. If the 5×10^4 N/m^2 (500 millibar) trough is still west of Florida, classify as D2, but if the trough is over, or east of, the peninsula, classify as B or GH. Sometimes, these fronts will move northward or become stationary near the latitude of Cape Canaveral. In these cases, the surface isobaric configuration is similar to pattern B, but the upper air more closely resembles a D pattern; i.e., a trough west of Florida. This situation is probably closer to D2 than to any other pattern and should be classified as such.

Figure 6, Pattern B

In the cool season, this pattern occurs between cold fronts and, under those circumstances, may persist for 1 or 2 days. In the fall, when anticyclones tend to stagnate over the Eastern United States, a type B pattern may persist for several days. In addition to the surface pattern typified by figure 6, B is also characterized by a 5×10^4 N/m^2 (500 millibar) trough position east of Florida.

Figure 7, Pattern GH

This cool season pattern usually occurs after a cold front has passed through Florida. Figure 7 shows a typical configuration, but one that is tending toward the B pattern.

Figure 8, Pattern E

A low-pressure center or trough of low pressure in the Gulf of Mexico is not sufficient reason to classify as pattern E, but if the low-level winds at the launch site are within the circulation of a low-pressure area in the Gulf, classify as E. The low pressure may be the result of tropical or extratropical weather systems. As figure 8 shows, type A3 may be similar to pattern E, but first determine the dominant influence on the low-level wind field in the launch area. Distinguishing correctly between E and A3 is important because E types produce precipitation and rather frequent onshore cloud transport.

Figure 9, Pattern LV

A typical light, variable wind situation is characterized by an extremely weak pressure gradient. There are other patterns that result in weak surface pressure gradients, but, for this classification, be sure that boundary layer winds are also light; i.e., approximately 5 m/sec (10 knots) or less. If the pressure difference does not exceed 10^2 N/m^2 (1 millibar) within 278 kilometers (150 nautical miles) of the launch area and if the boundary layer winds are 5 m/sec (10 knots) or less, classify as LV.

CONCLUDING REMARKS

The twin problems of predicting ground-level concentrations of hydrogen chloride (HCl) and the groundpath of the effluent cloud resulting from the launch of the Space Shuttle from Cape Canaveral, Florida, were considered in this study. Because these factors are potentially hazardous to both plant and animal life in the area, accurate estimates concerning these concentrations and the launch-cloud transport 24 to 48 hours before launch were deemed potentially valuable to the launch personnel.

To this end, concentration estimates of various exhaust-cloud constituents were made, and predicted concentrations of HCl were compared with ground-level measurements of HCl made during several Titan III-C launches. Also, nine weather patterns basic to the Cape Canaveral area were identified and evaluated as to the probability of pattern occurrence, onshore/alongshore cloud transport, and precipitation associated with the latter. These data were tabulated together with other information from the National Weather Service, and tables, figures, and maps were prepared showing the HCl concentrations that could be expected and the probable direction of the launch cloud.

One finding was that peak concentrations of HCl associated with two of the weather patterns might sometimes exceed the allowable limit and therefore should be considered, even though these two patterns usually moved offshore. Also, the highest concentration of HCl was usually found to occur within 6000 meters of the launch site. The diurnal variations were not found to be significant. Rather, synoptic meteorology was considered to be of more potential value to the launch team. From the maps and figures, data are available to show where the launch-cloud exhaust will go approximately 90 percent of the time within a 3-hour period.

By identifying and classifying current weather patterns and comparing them with prognostic charts and by employing the methods and suggestions presented in this study, practical estimates concerning probable HCl concentrations and the groundpath of the effluent cloud may be made.

Lyndon B. Johnson Space Center
National Aeronautics and Space Administration
Houston, Texas, April 11, 1980
152-85-00-00-72

TABLE I.- PROBABILITY OF PATTERN OCCURRENCE WITHOUT REGARD TO TIME OF DAY

Weather pattern	Months												Yearly average
	Jan.	Feb.	Mar.	Apr.	May	June	July	Aug.	Sept.	Oct.	Nov.	Dec.	
A1	0.113	0.074	0.128	0.186	0.266	0.236	0.227	0.296	0.376	0.252	0.137	0.148	0.205
A2	.149	.093	.179	.138	.120	.145	.262	.214	.070	.044	.081	.141	.137
A3	.076	.087	.104	.129	.118	.181	.188	.117	.024	.018	.019	.047	.092
D1	.104	.134	.142	.124	.090	.093	.024	.030	.062	.078	.139	.136	.096
D2	.134	.178	.126	.076	.058	.020	.012	.007	.029	.054	.124	.120	.076
B	.206	.152	.101	.120	.123	.039	.032	.061	.226	.332	.264	.174	.152
GH	.097	.175	.136	.088	.061	.029	.007	.022	.013	.076	.123	.139	.079
E	.036	.032	.036	.016	.033	.056	.029	.059	.042	.053	.027	.021	.037
LV	.080	.075	.046	.120	.118	.171	.215	.179	.129	.076	.080	.075	.114

TABLE II.- PROBABILITY OF ONSHORE/ALONGSHORE CLOUD TRANSPORT WITHOUT REGARD TO TIME OF DAY

Weather pattern	Months												Yearly average
	Jan.	Feb.	Mar.	Apr.	May	June	July	Aug.	Sept.	Oct.	Nov.	Dec.	
A1	0.714	0.640	0.847	0.936	0.874	0.944	0.904	0.934	0.990	0.986	0.913	0.883	0.913
A2	.349	.095	.452	.431	.500	.451	.502	.505	.712	.579	.544	.508	.467
A3	.030	.051	.067	.056	.088	.053	.123	.068	.050	.062	.312	.125	.078
D1	.067	.022	.024	.029	.051	.090	.286	.154	.096	.206	.111	.039	.074
D2	.103	.066	.028	.062	.120	.176	.400	.500	.375	.213	.135	.154	.119
B	.788	.884	.909	.852	.850	.727	.893	.868	.821	.944	.887	.748	.857
GH	.202	.126	.119	.216	.283	.292	1.000	.263	.546	.530	.184	.116	.210
E	.323	.318	.323	.077	.345	.617	.480	.510	.600	.652	.348	.389	.507
LV	.333	.176	.525	.406	.412	.535	.471	.594	.509	.515	.239	.369	.452

TABLE III.- PROBABILITY OF PRECIPITATION AND ONSHORE/ALONGSHORE CLOUD TRANSPORT WITHOUT REGARD TO TIME OF DAY

Weather pattern	Months												Yearly average
	Jan.	Feb.	Mar.	Apr.	May	June	July	Aug.	Sept.	Oct.	Nov.	Dec.	
A1	0.027	0.000	0.033	0.049	0.073	0.091	0.070	0.094	0.149	0.148	0.048	0.071	0.090
A2	.022	.000	.014	.000	.038	.056	.061	.021	.095	.000	.108	.048	.042
A3	.000	.000	.000	.000	.000	.125	.050	.143	.000	.000	.000	.000	.041
D1	.000	.000	.000	.667	.250	.571	.167	.000	.000	.071	.000	.000	.127
D2	.000	.125	.000	.000	.167	.250	.750	.333	.111	.300	.000	.062	.130
B	.043	.077	.012	.023	.044	.125	.080	.022	.173	.176	.076	.017	.089
GH	.000	.000	.000	.000	.067	.000	.000	.000	.000	.057	.000	.000	.018
E	.600	.143	.300	1.000	.148	.586	.250	.077	.286	.233	.375	.286	.293
LV	.000	.000	.000	.024	.000	.078	.057	.065	.000	.029	.000	.000	.036

TABLE IV.- SUMMARY OF DIFFUSION ESTIMATES FOR 79 CASE DAYS

Diffusion variables	Model 4		Model 3	
	Morning	Afternoon	Morning	Afternoon
Pattern A1				
χ, p/m	0.653	0.856	0.824	1.034
χ_M, p/m	1.486	1.529	2.466	1.967
D, m	4500	6000	(a)	(a)
P_1, percent	1.000	0.900	(b)	(b)
Pattern A2				
χ, p/m	0.515	0.457	0.543	0.486
χ_M, p/m	1.725	0.843	2.019	0.830
D, m	2219	4722	(a)	(a)
P_1, percent	0.500	0.444	(b)	(b)
Pattern A3				
χ, p/m	0.533	0.498	0.544	0.607
χ_M, p/m	0.911	0.752	0.882	0.898
D, m	3125	6562	(a)	(a)
P_1, percent	0.000	0.000	(b)	(b)
Pattern D1				
χ, p/m	0.887	0.698	1.132	0.950
χ_M, p/m	1.504	1.897	2.823	2.919
D, m	5062	5000	(a)	(a)
P_1, percent	0.000	0.000	(b)	(b)
Pattern D2				
χ, p/m	0.672	0.675	0.752	0.771
χ_M, p/m	1.709	1.105	1.968	1.385
D, m	3528	3667	(a)	(a)
P_1, percent	0.222	0.333	(b)	(b)
Pattern B				
χ, p/m	0.636	0.523	0.693	0.583
χ_M, p/m	1.667	0.787	1.967	1.133
D, m	4969	5611	(a)	(a)
P_1, percent	0.750	0.444	(b)	(b)
Pattern GH				
χ, p/m	0.862	0.866	1.0814	1.195
χ_M, p/m	2.526	2.325	2.624	2.112
D, m	5786	6388	(a)	(a)
P_1, percent	0.273	0.400	(b)	(b)
Pattern E				
χ, p/m	0.795	0.462	1.002	0.477
χ_M, p/m	1.017	0.690	1.487	0.773
D, m	5312	4688	(a)	(a)
P_1, percent	0.200	0.200	(b)	(b)
Pattern LV				
χ, p/m	0.383	0.535	0.376	0.652
χ_M, p/m	0.665	1.276	0.604	1.604
D, m	932	6050	(a)	(a)
P_1, percent	0.545	0.500	(b)	(b)

[a]Not given.
[b]Not given. Data considered unreliable.

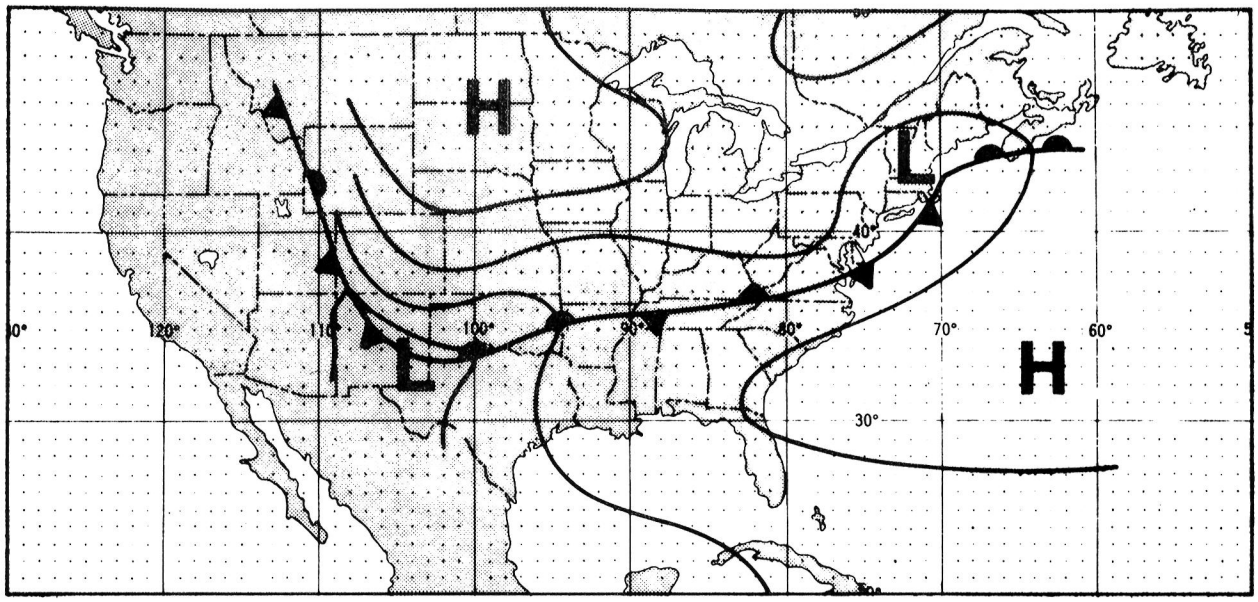

Probabilities	Months												Yearly average
	Jan.	Feb.	Mar.	Apr.	May	June	July	Aug.	Sept.	Oct.	Nov.	Dec.	
P	0.113	0.074	0.128	0.186	0.266	0.236	0.227	0.296	0.376	0.252	0.137	0.148	0.205
P_1	.714	.640	.847	.936	.874	.944	.904	.934	.990	.986	.913	.883	.913
P_2	.027	.000	.033	.049	.073	.091	.070	.094	.149	.148	.048	.071	.090

(a) Weather map, pattern A1.

Figure 1.- Isobaric weather map for pattern A1 and sketch showing movement of launch-exhaust cloud (where ddd = 121.4, V = 6.0, S_d = 59.62, χ = 0.755, χ_M = 1.529, and D = 5250).

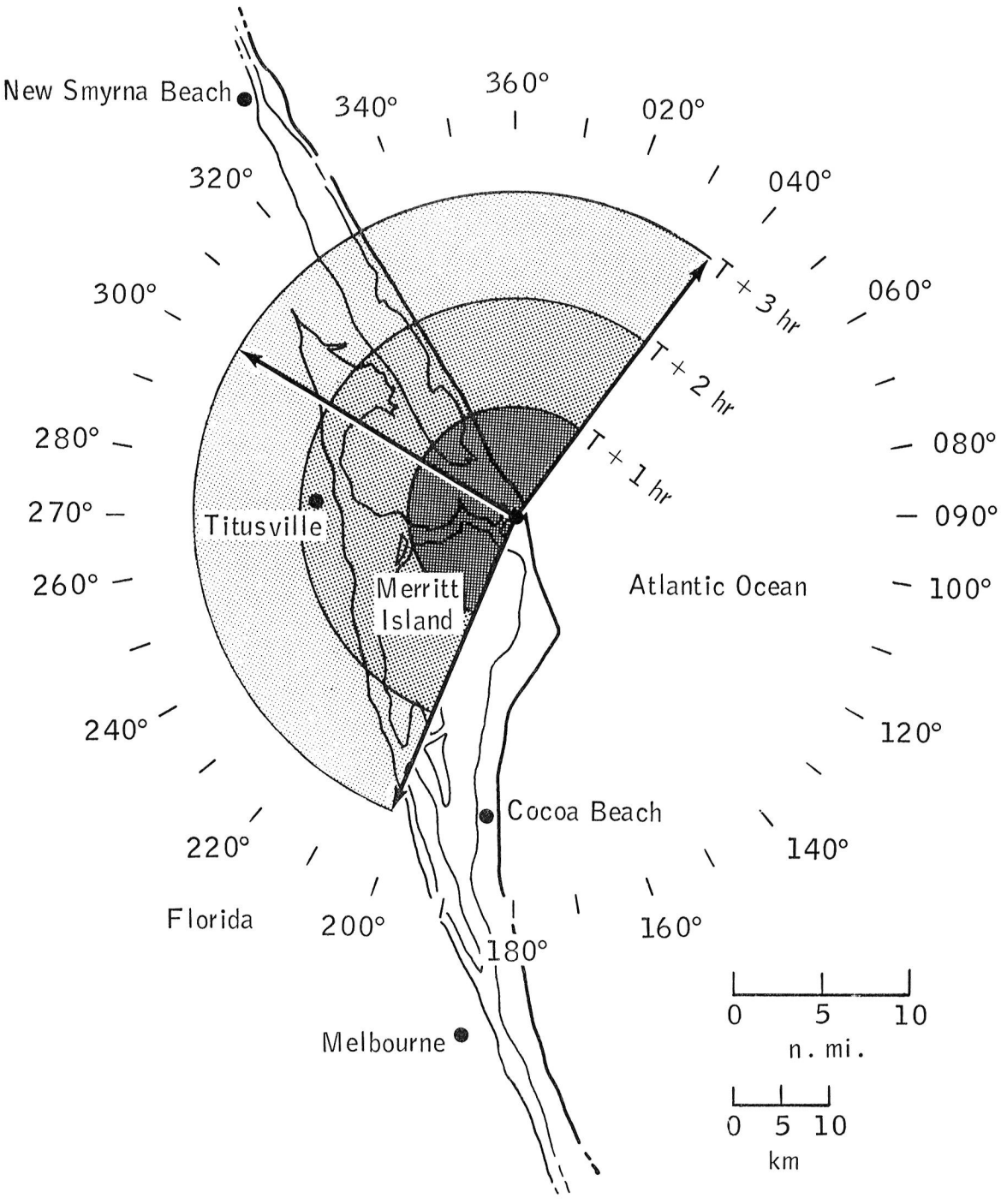

(b) Launch-exhaust cloud movement.

Figure 1.- Concluded.

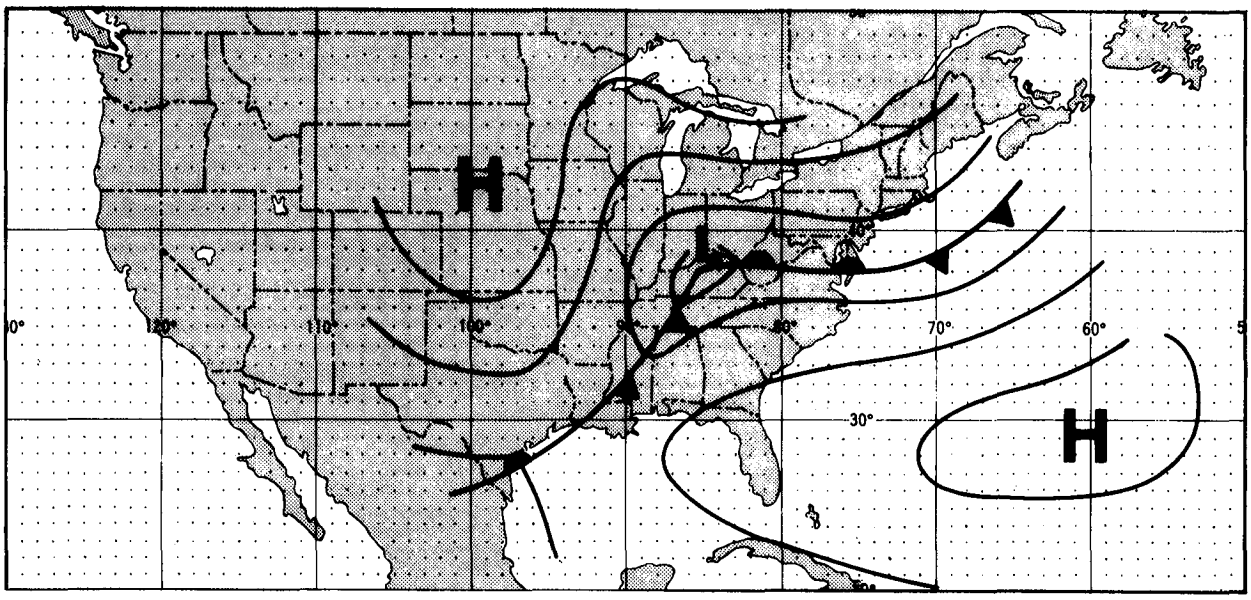

Probabilities	Months												Yearly average
	Jan.	Feb.	Mar.	Apr.	May	June	July	Aug.	Sept.	Oct.	Nov.	Dec.	
P	0.149	0.093	0.179	0.138	0.120	0.145	0.262	0.214	0.070	0.044	0.081	0.141	0.137
P_1	.349	.095	.452	.431	.500	.451	.502	.505	.712	.579	.544	.508	.467
P_2	.022	.000	.014	.000	.038	.056	.061	.021	.095	.000	.108	.048	.042

(a) Weather map, pattern A2.

Figure 2.- Isobaric weather map for pattern A2 and sketch showing movement of launch-exhaust cloud (where ddd = 178.2, V = 5.5, S_d = 70.16, χ = 0.486, χ_M = 1.725, and D = 3470).

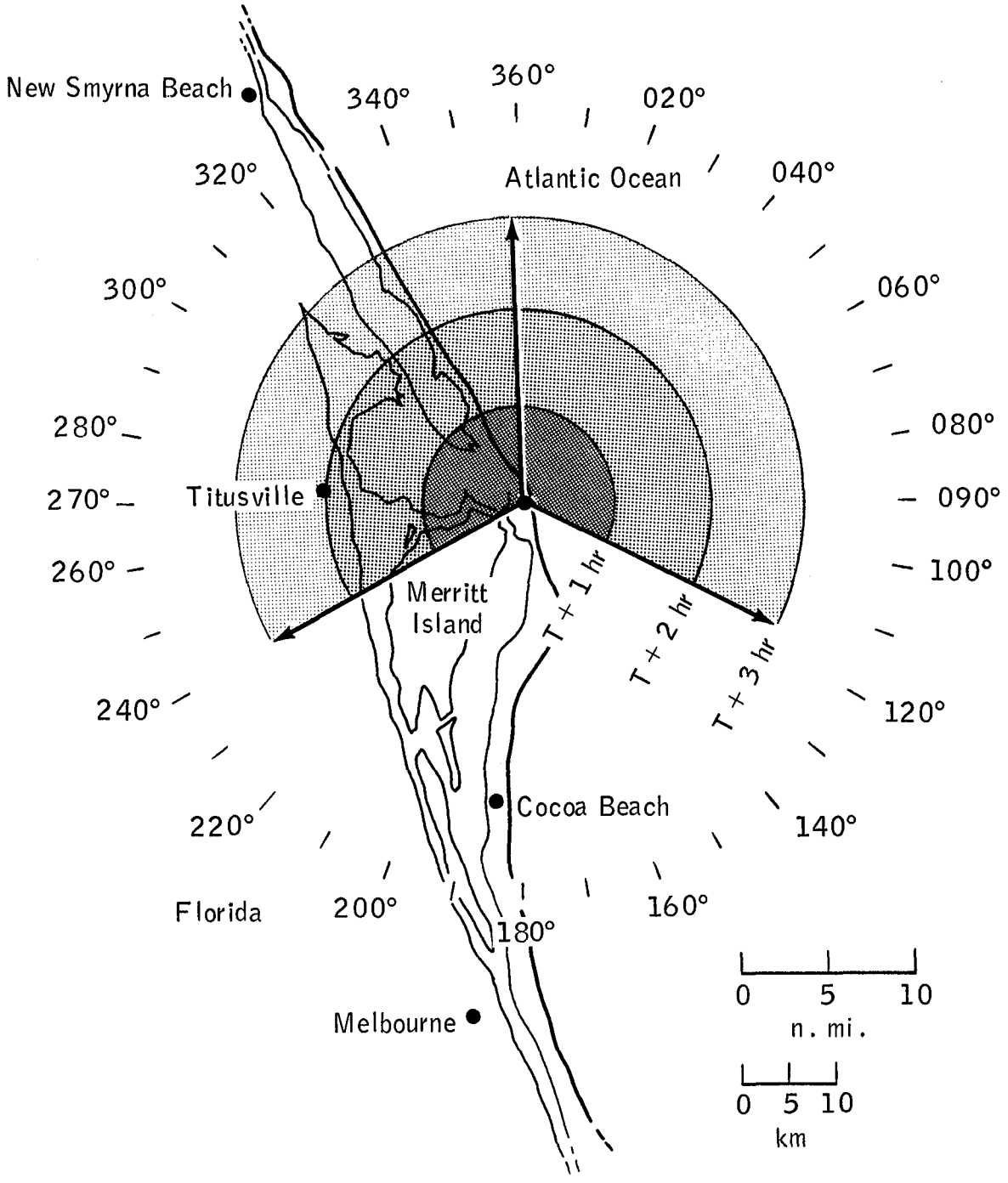

(b) Launch-exhaust cloud movement.

Figure 2.- Concluded.

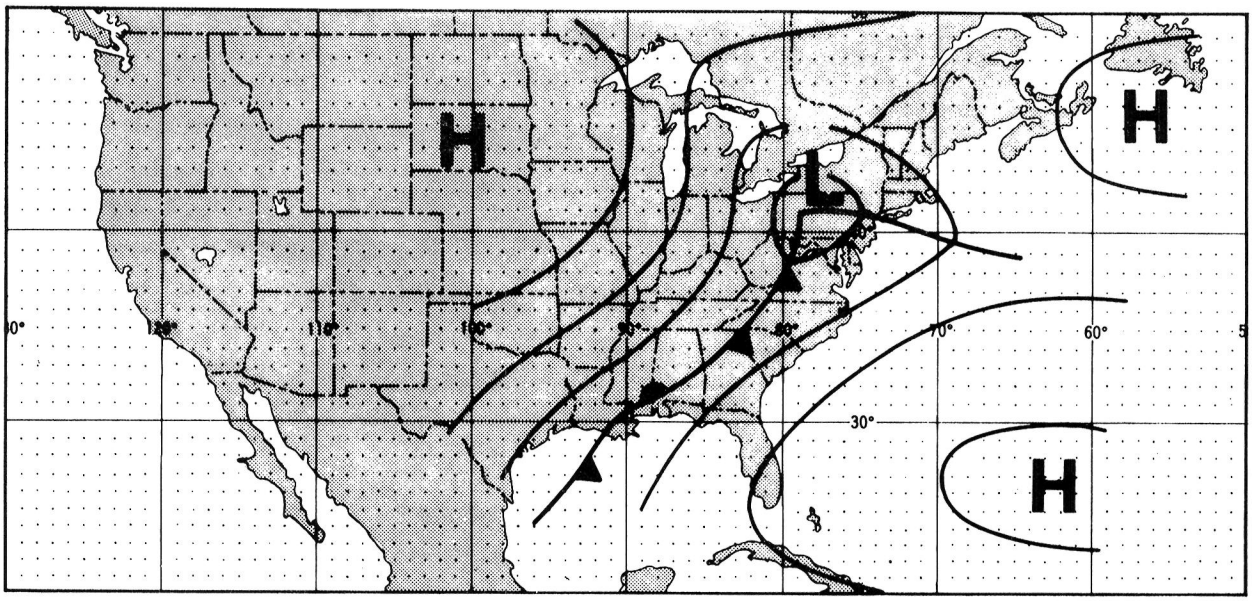

Probabilities	Months												Yearly average
	Jan.	Feb.	Mar.	Apr.	May	June	July	Aug.	Sept.	Oct.	Nov.	Dec.	
P	0.076	0.087	0.104	0.129	0.118	0.181	0.188	0.117	0.024	0.018	0.019	0.047	0.092
P_1	.030	.051	.067	.056	.088	.053	.123	.068	.050	.062	.312	.125	.078
P_2	.000	.000	.000	.000	.000	.125	.050	.143	.000	.000	.000	.000	.041

(a) Weather map, pattern A3.

Figure 3.- Isobaric weather map for pattern A3 and sketch showing movement of launch-exhaust cloud (where ddd = 230.8, V = 7.6, S_d = 52.66, χ = 0.516, χ_M = 0.911, and D = 4844).

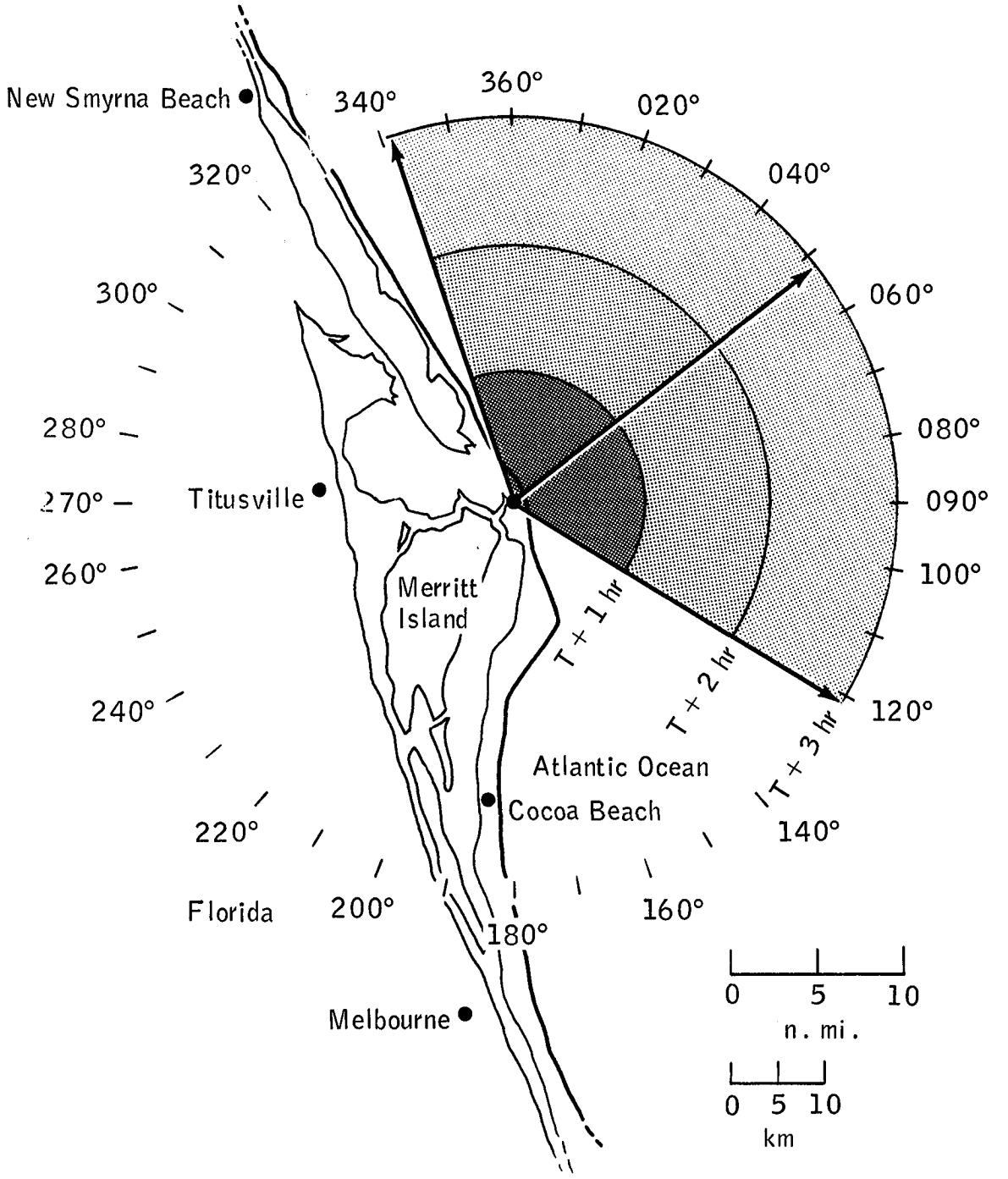

(b) Launch-exhaust cloud movement.

Figure 3.- Concluded.

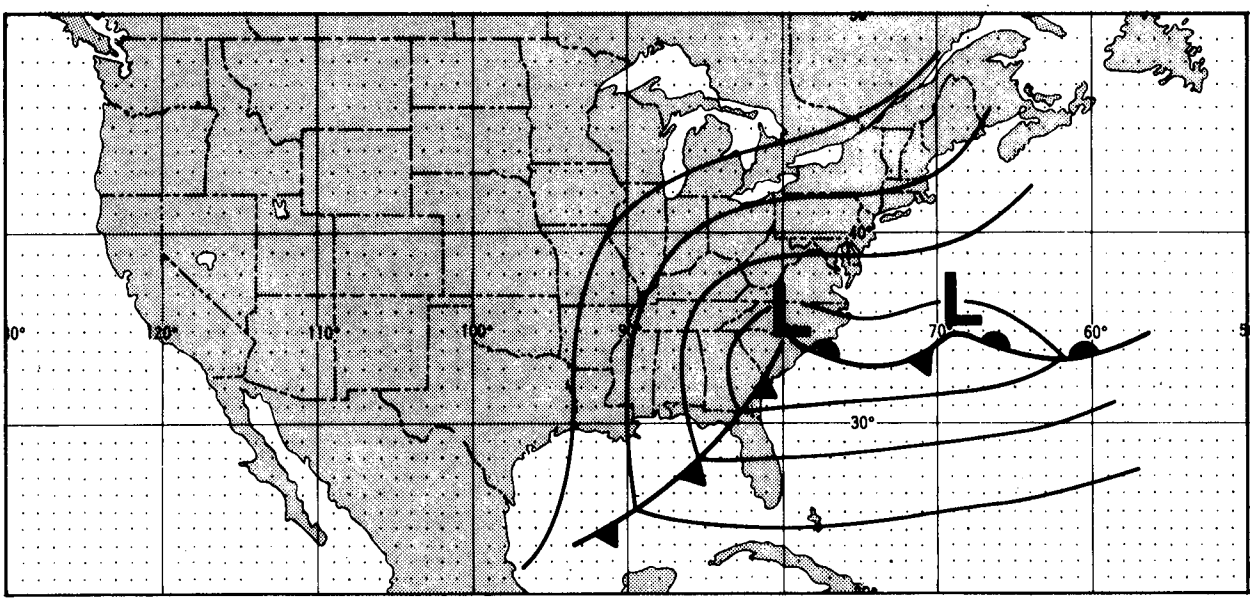

Probabilities	Months												Yearly average
	Jan.	Feb.	Mar.	Apr.	May	June	July	Aug.	Sept.	Oct.	Nov.	Dec.	
P	0.104	0.134	0.142	0.124	0.090	0.093	0.024	0.030	0.062	0.078	0.139	0.136	0.096
P_1	.067	.022	.024	.029	.051	.090	.286	.154	.096	.206	.111	.039	.074
P_2	.000	.000	.000	.667	.250	.571	.167	.000	.000	.071	.000	.000	.127

(a) Weather map, pattern D1.

Figure 4.- Isobaric weather map for pattern D1 and sketch showing movement of launch-exhaust cloud (where ddd = 231.4, V = 10.7, S_d = 59.04, χ = 0.792, χ_M = 1.897, and D = 5031).

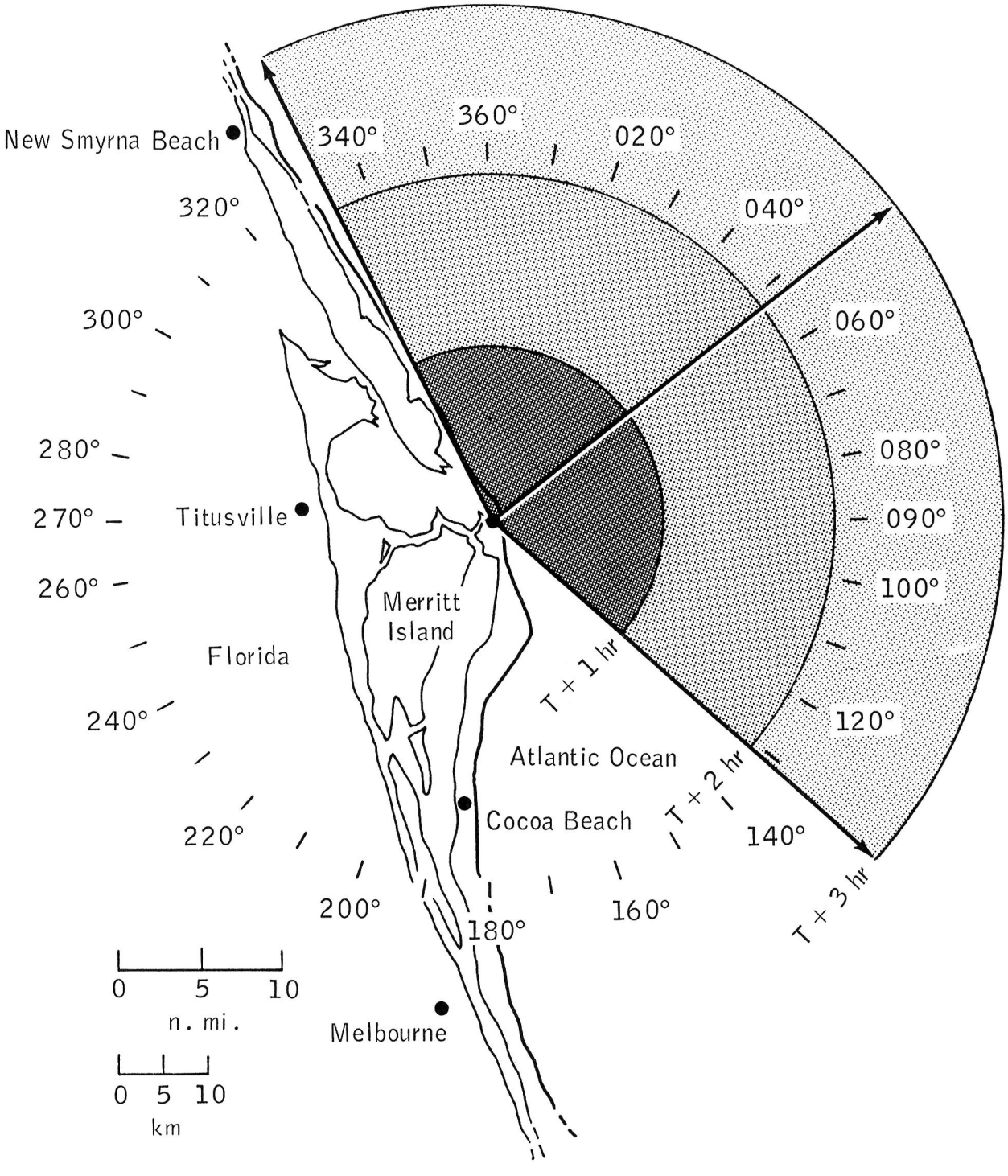

(b) Launch-exhaust cloud movement.

Figure 4.- Concluded.

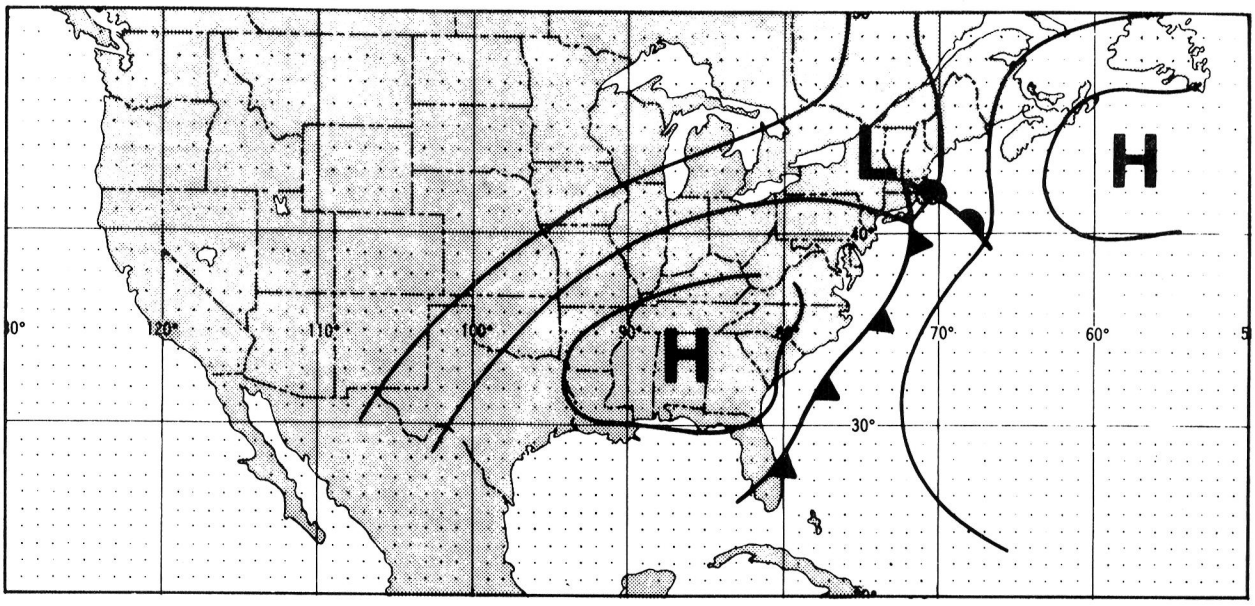

Probabilities	Months												Yearly average
	Jan.	Feb.	Mar.	Apr.	May	June	July	Aug.	Sept.	Oct.	Nov.	Dec.	
P	0.134	0.178	0.126	0.076	0.058	0.020	0.012	0.007	0.029	0.054	0.124	0.120	0.076
P_1	.103	.066	.028	.062	.120	.176	.400	.500	.375	.213	.135	.154	.119
P_2	.000	.125	.000	.000	.167	.250	.750	.333	.111	.300	.000	.062	.130

(a) Weather map, pattern D2.

Figure 5.- Isobaric weather map for pattern D2 and sketch showing movement of launch-exhaust cloud (where ddd = 255.4, V = 10.8, S_d = 73.79, χ = 0.674, χ_M = 1.709, and D = 3598).

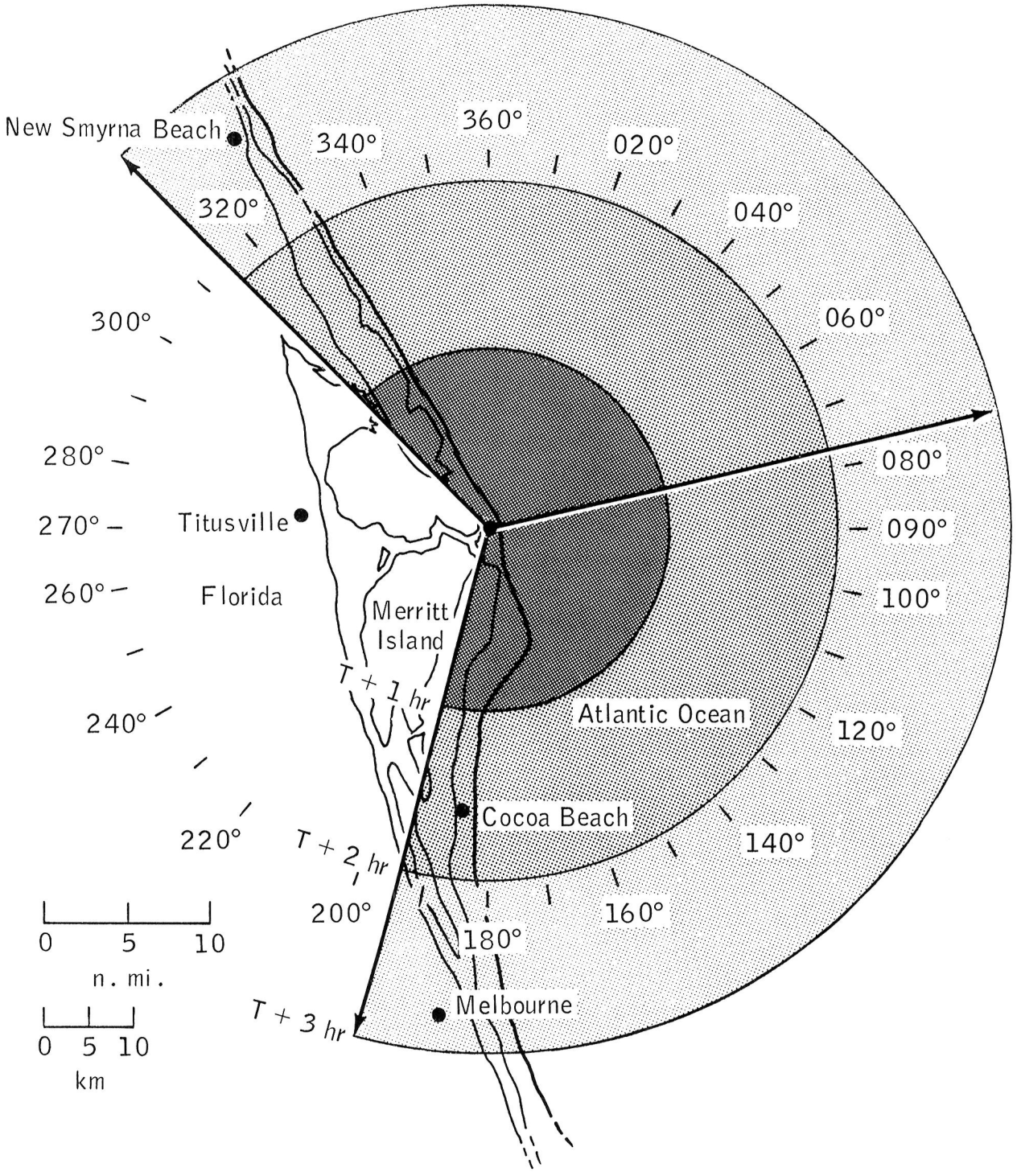

(b) Launch-exhaust cloud movement.

Figure 5.- Concluded.

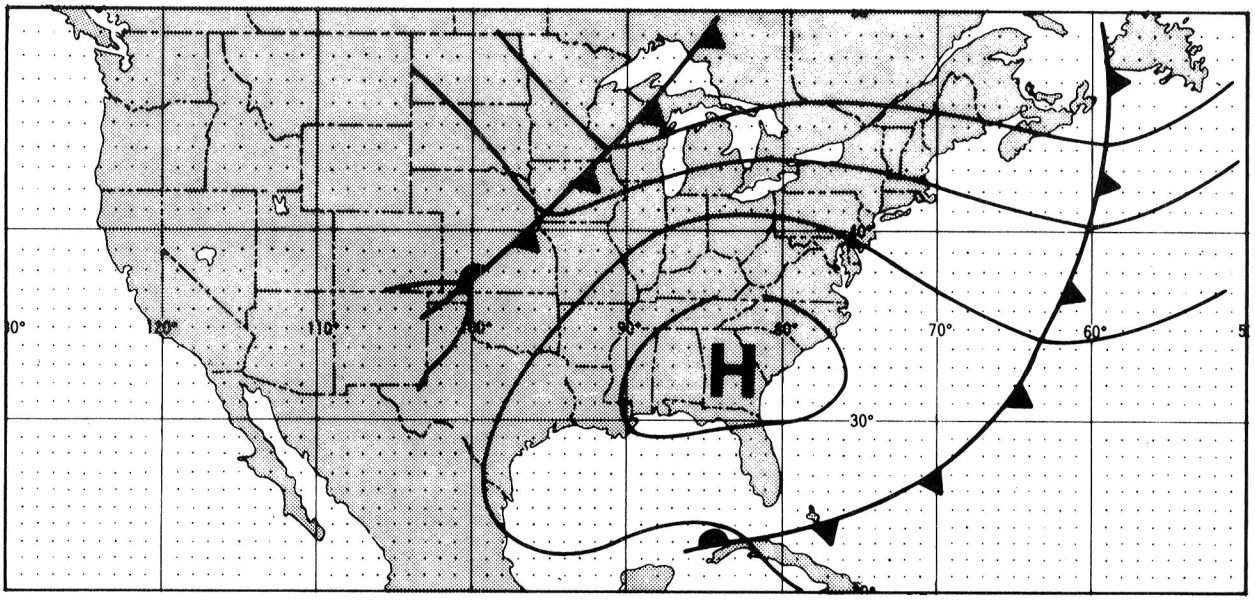

Probabilities	Months												Yearly average
	Jan.	Feb.	Mar.	Apr.	May	June	July	Aug.	Sept.	Oct.	Nov.	Dec.	
P	0.206	0.152	0.101	0.120	0.123	0.039	0.032	0.061	0.226	0.332	0.264	0.174	0.152
P_1	.788	.884	.909	.852	.850	.727	.893	.868	.821	.944	.887	.748	.857
P_2	.043	.077	.012	.023	.044	.125	.080	.022	.173	.176	.076	.017	.089

(a) Weather map, pattern B.

Figure 6.- Isobaric weather map for pattern B and sketch showing movement of launch-exhaust cloud (where ddd = 065.2, V = 6.6, S_d = 70.75, χ = 0.580, χ_M = 1.667, and D = 5290).

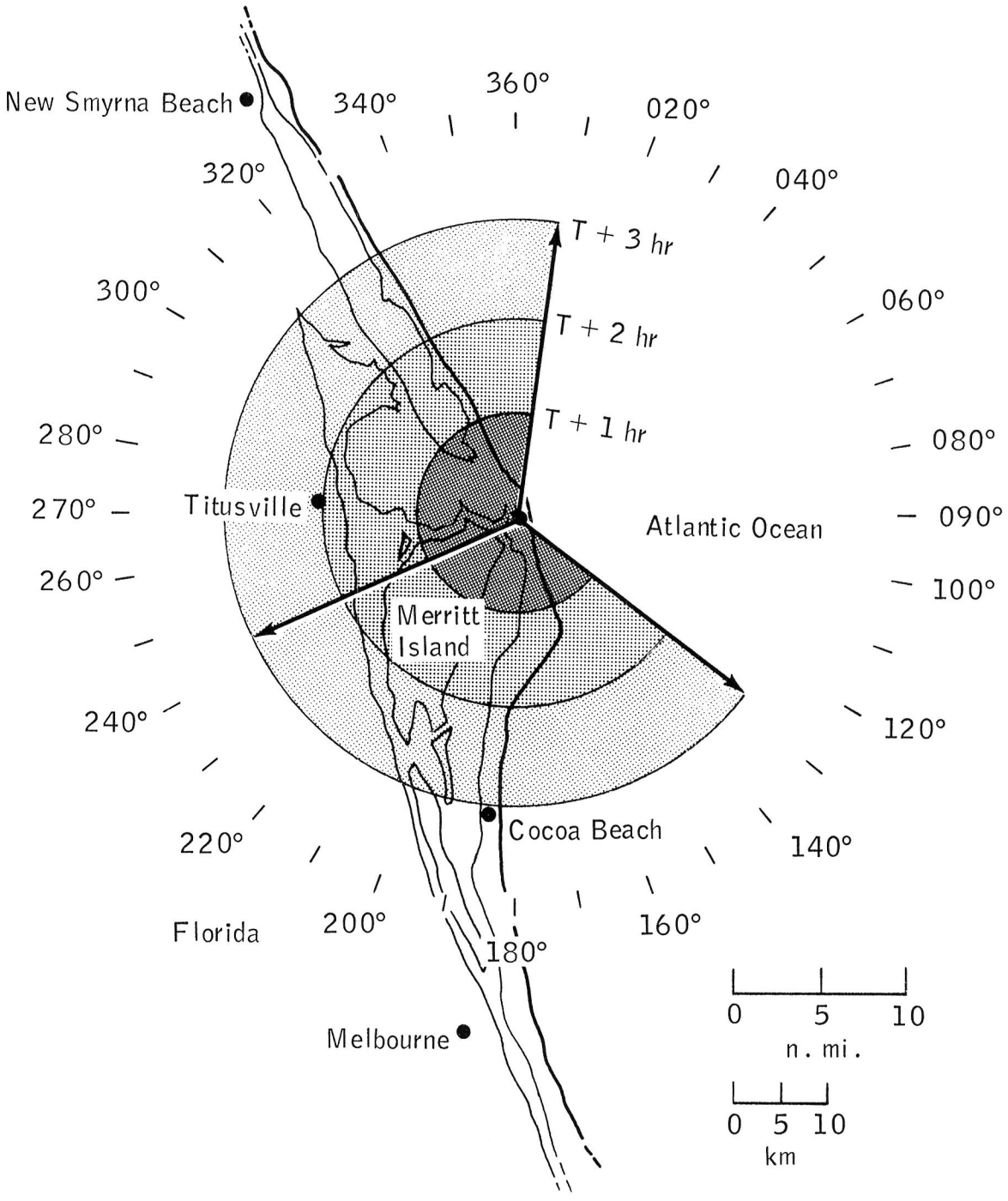

(b) Launch-exhaust cloud movement.

Figure 6.- Concluded.

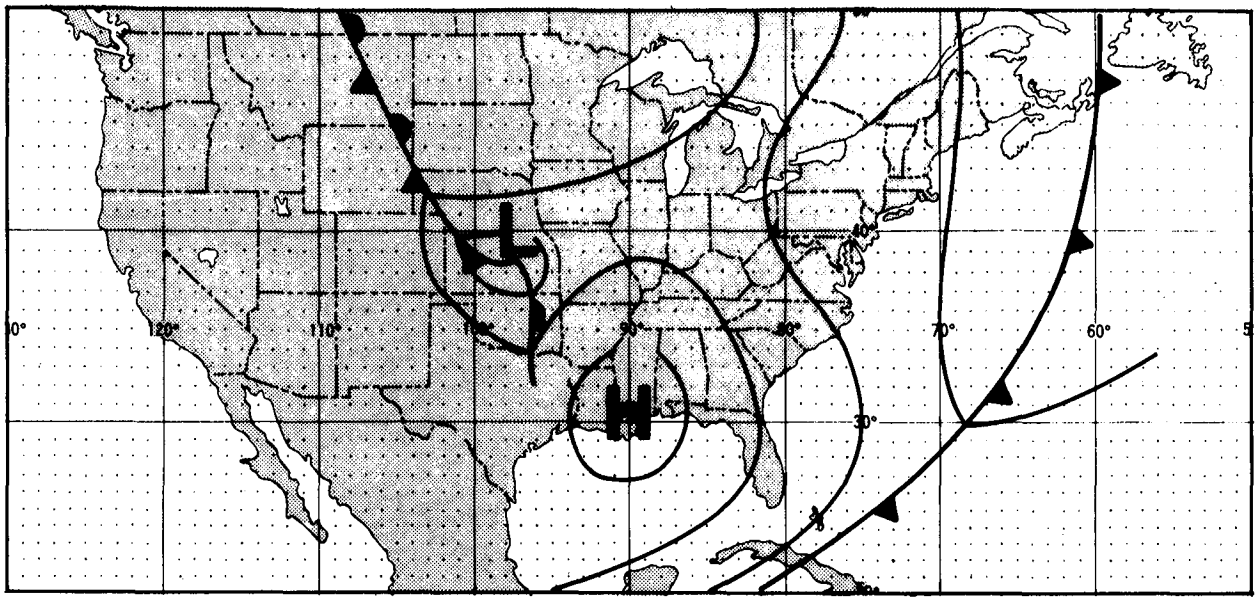

Probabilities	Months												Yearly average
	Jan.	Feb.	Mar.	Apr.	May	June	July	Aug.	Sept.	Oct.	Nov.	Dec.	
P	0.097	0.175	0.136	0.088	0.061	0.029	0.007	0.022	0.013	0.076	0.123	0.139	0.079
P_1	.202	.126	.119	.216	.283	.292	1.000	.263	.546	.530	.184	.116	.210
P_2	.000	.000	.000	.000	.067	.000	.000	.000	.000	.057	.000	.000	.018

(a) Weather map, pattern GH.

Figure 7.- Isobaric weather map for pattern GH and sketch showing movement of launch-exhaust cloud (where ddd = 292.6, V = 10.4, S_d = 68.86, χ = 0.864, χ_M = 2.526, and D = 6087).

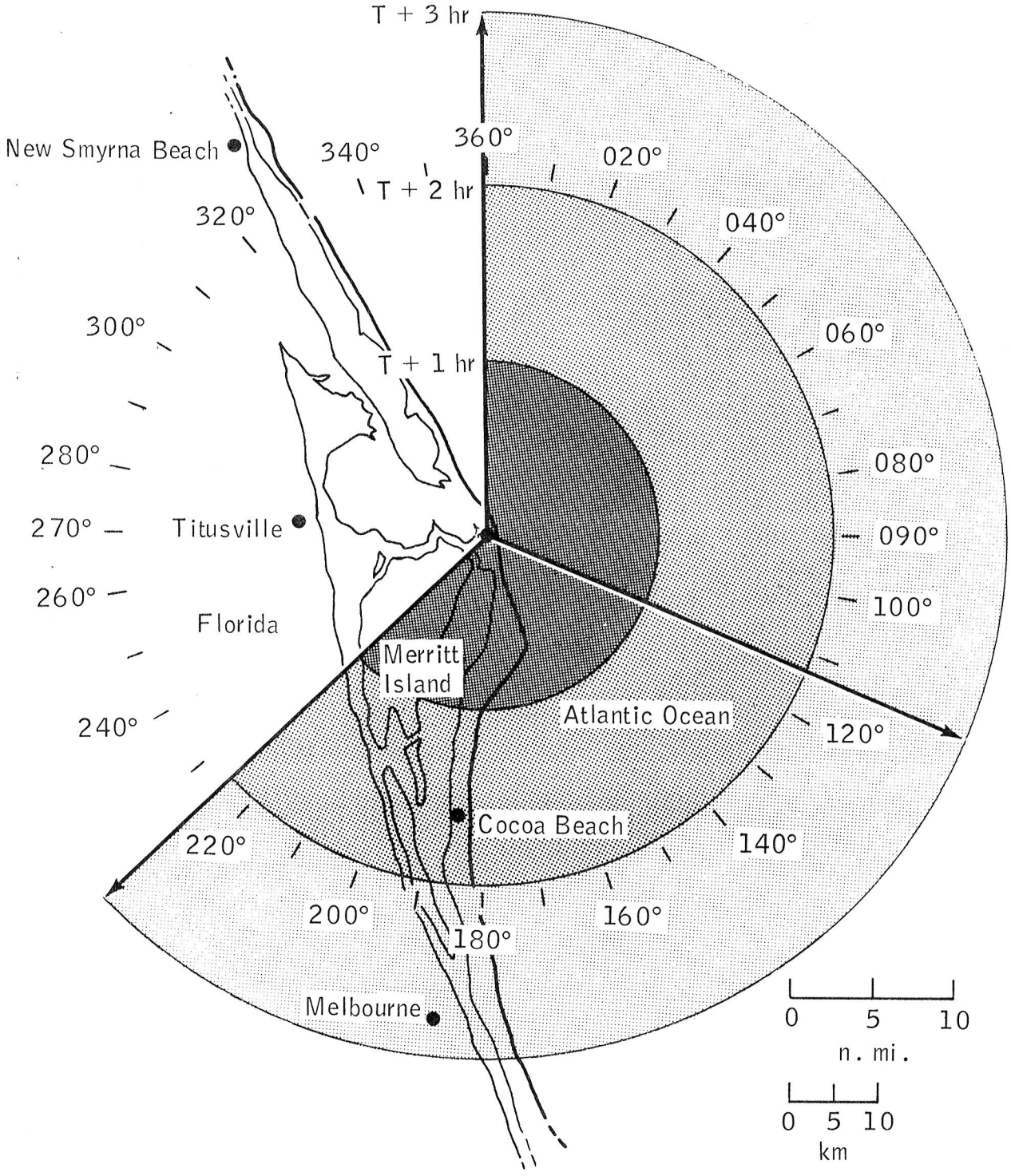

(b) Launch-exhaust cloud movement.

Figure 7.- Concluded.

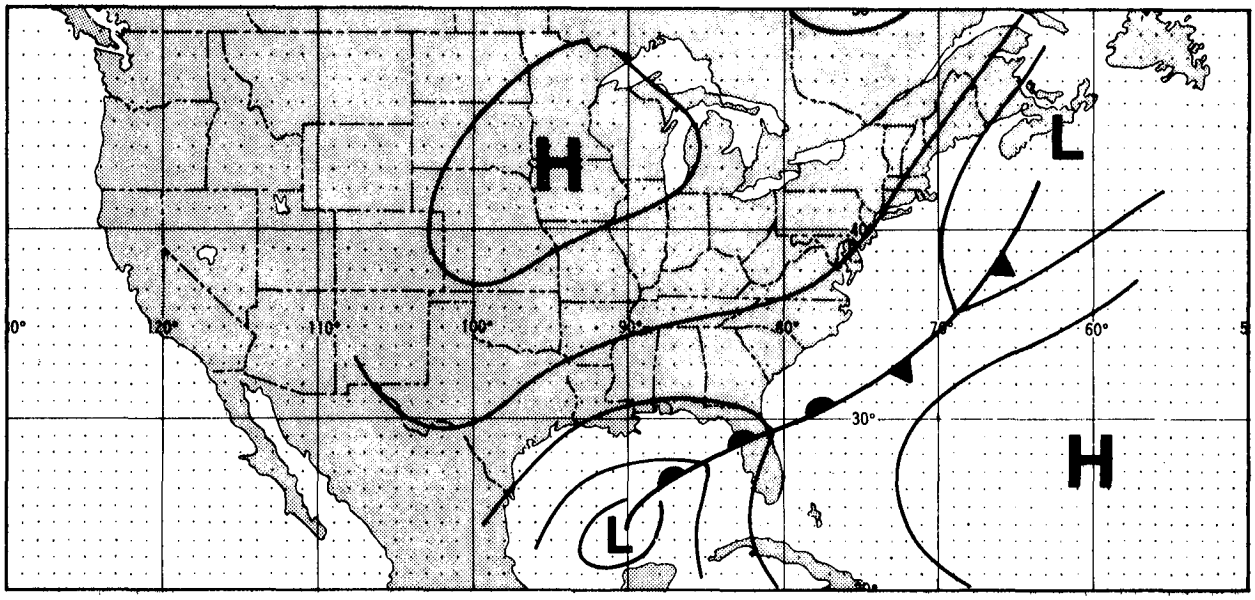

Probabilities	Months												Yearly average
	Jan.	Feb.	Mar.	Apr.	May	June	July	Aug.	Sept.	Oct.	Nov.	Dec.	
P	0.036	0.032	0.036	0.016	0.033	0.056	0.029	0.059	0.042	0.053	0.027	0.021	0.037
P_1	.323	.318	.323	.077	.345	.617	.480	.510	.600	.652	.348	.389	.507
P_2	.600	.143	.300	1.000	.148	.586	.250	.077	.286	.233	.375	.286	.293

(a) Weather map, pattern E.

Figure 8.- Isobaric weather map for pattern E and sketch showing movement of launch-exhaust cloud (where ddd = 179.2, V = 10.0, S_d = 54.48, χ = 0.628, χ_M = 1.017, and D = 5000).

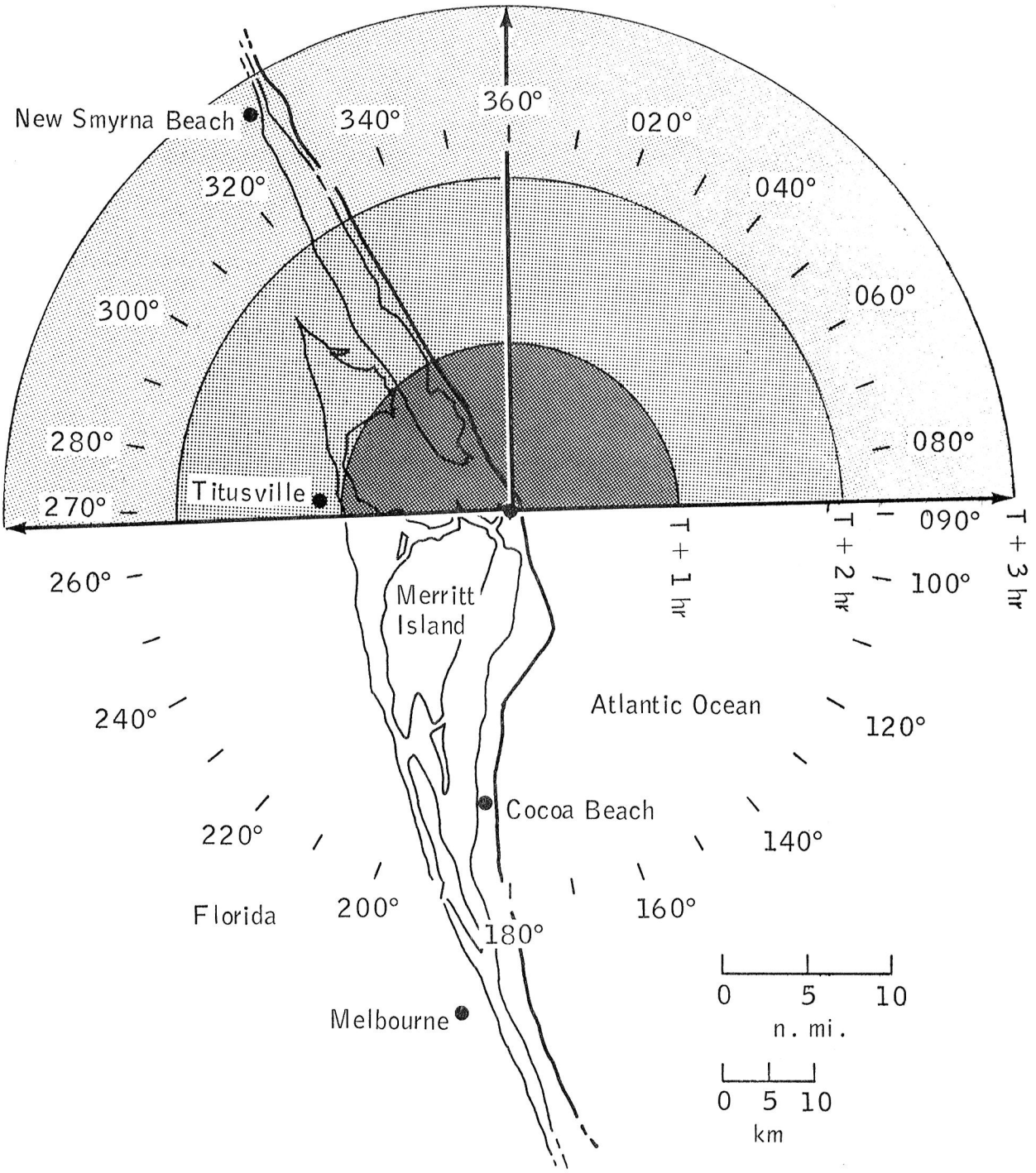

(b) Launch-exhaust cloud movement.

Figure 8.- Concluded.

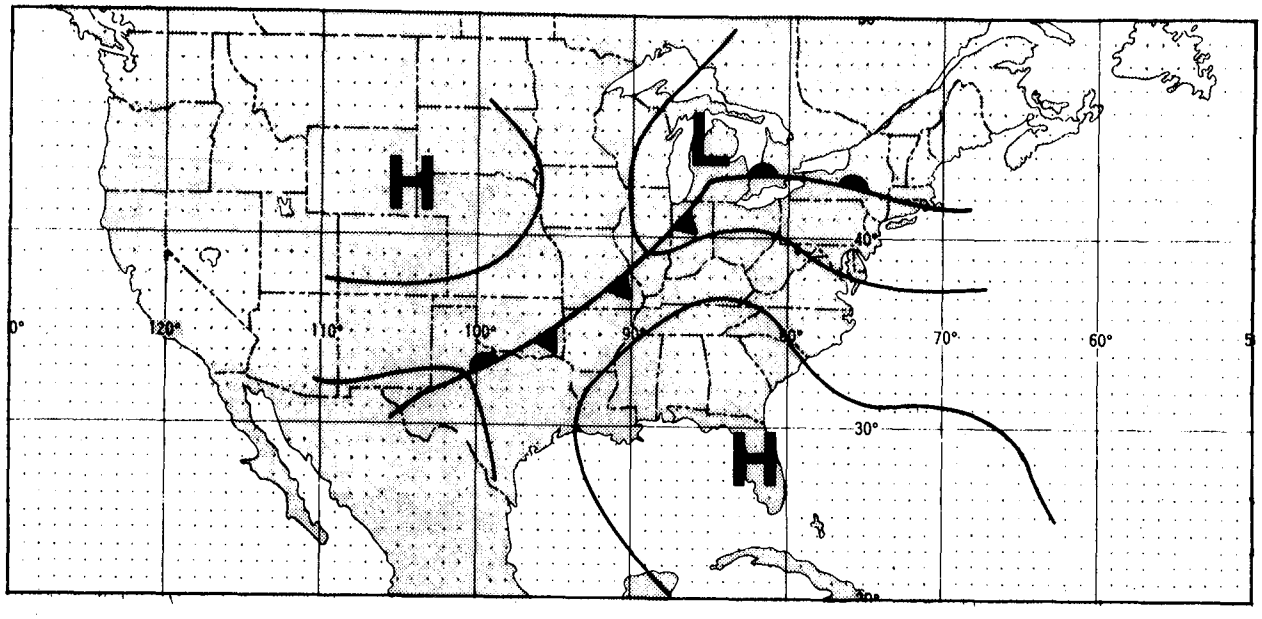

Probabilities	Months												Yearly average
	Jan.	Feb.	Mar.	Apr.	May	June	July	Aug.	Sept.	Oct.	Nov.	Dec.	
P	0.080	0.075	0.046	0.120	0.118	0.171	0.215	0.179	0.129	0.076	0.080	0.075	0.114
P_1	.333	.176	.525	.406	.412	.535	.471	.594	.509	.515	.239	.369	.452
P_2	.000	.000	.000	.024	.000	.078	.057	.065	.000	.029	.000	.000	.036

(a) Weather map, pattern LV.

Figure 9.- Isobaric weather map for pattern LV and sketch showing movement of launch-exhaust cloud (where ddd = 174.8, V = 4.5, S_d = 105.21, χ = 0.459, χ_M = 1.276, and D = 3491).

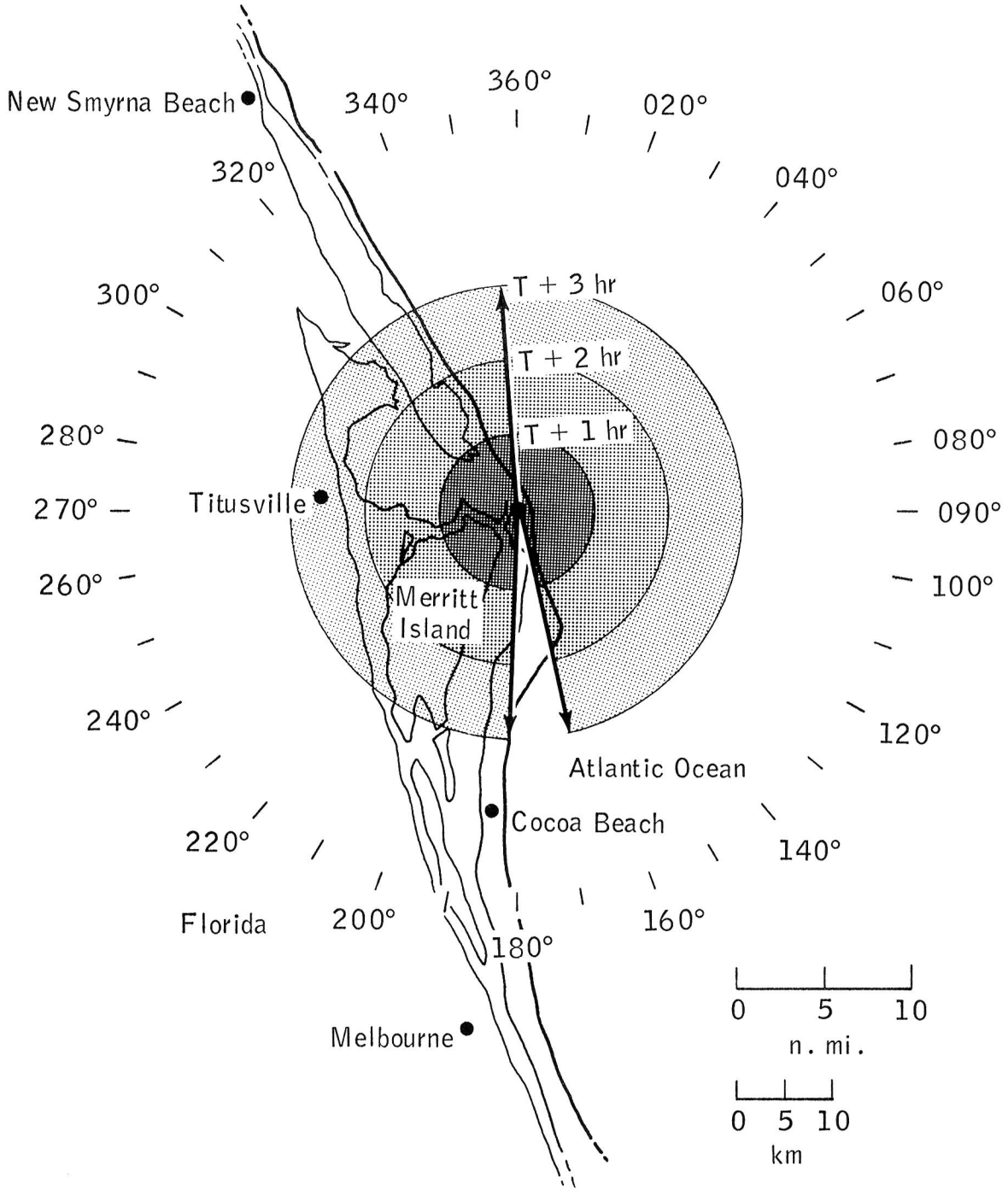

(b) Launch-exhaust cloud movement.

Figure 9.- Concluded.

APPENDIX

DIURNAL VARIATIONS FOR THE NINE BASIC WEATHER PATTERNS

Diurnal variation statistics compiled for this study of the nine basic weather patterns are presented in tables V to XIII of this appendix. These data are based on four readings per day and are computed by month to show the probabilities for the occurrence of each basic weather pattern, onshore/alongshore cloud transport, and precipitation associated with the cloud transport.

TABLE V.- PATTERN A1

G.m.t.	Months												Yearly average
	Jan.	Feb.	Mar.	Apr.	May	June	July	Aug.	Sept.	Oct.	Nov.	Dec.	
						Probability of occurrence							
00:00	0.134	0.064	0.129	0.171	0.276	0.200	0.207	0.286	0.390	0.254	0.162	0.148	0.204
06:00	.101	.082	.143	.186	.286	.252	.244	.304	.381	.240	.138	.138	.210
12:00	.101	.082	.120	.195	.263	.267	.263	.309	.386	.254	.119	.157	.212
18:00	.115	.065	.120	.190	.240	.224	.194	.286	.348	.263	.129	.148	.195
						Probability of onshore/alongshore cloud transport							
00:00	0.552	0.546	0.893	0.944	0.917	0.952	0.822	0.936	0.988	1.000	0.912	1.000	0.882
06:00	.773	.643	.839	.974	.952	.943	.906	.939	.988	1.000	1.000	.867	.928
12:00	.864	.643	.808	.902	.947	.911	.912	.910	.988	.964	.840	.794	.906
18:00	.720	.727	.846	.925	.962	.979	.976	.952	.973	.982	.889	.875	.933
						Probability of precipitation and onshore/alongshore cloud transport							
00:00	0.000	0.000	0.042	0.029	0.054	0.125	0.094	0.107	0.171	0.091	0.000	0.094	0.087
06:00	.000	.000	.038	.053	.102	.040	.064	.129	.188	.212	.103	.077	.107
12:00	.050	.000	.000	.057	.074	.098	.038	.066	.075	.132	.000	.111	.070
18:00	.050	.000	.048	.054	.600	.109	.098	.073	.167	.161	.083	.000	.094

TABLE VI.- PATTERN A2

G.m.t	Months												Yearly average
	Jan.	Feb.	Mar.	Apr.	May	June	July	Aug.	Sept.	Oct.	Nov.	Dec.	
						Probability of occurrence							
00:00	0.143	0.106	0.166	0.162	0.097	0.148	0.272	0.258	0.086	0.046	0.095	0.124	0.143
06:00	.170	.082	.175	.152	.124	.152	.235	.212	.081	.055	.081	.157	.141
12:00	.166	.077	.184	.110	.120	.124	.249	.175	.038	.042	.071	.148	.126
18:00	.115	.106	.189	.129	.138	.157	.281	.212	.076	.032	.076	.134	.138
						Probability of onshore/alongshore cloud transport							
00:00	0.258	0.167	0.389	0.412	0.524	0.484	0.542	0.571	0.500	0.600	0.500	0.518	0.465
06:00	.270	.071	.395	.469	.593	.344	.471	.478	.882	.750	.647	.500	.465
12:00	.306	.077	.400	.348	.461	.385	.426	.368	.500	.333	.467	.406	.381
18:00	.640	.056	.610	.482	.433	.546	.574	.565	.875	.571	.562	.621	.550
						Probability of precipitation and onshore/alongshore cloud transport							
00:00	0.000	0.000	0.000	0.000	0.091	0.133	0.156	0.031	0.000	0.000	0.100	0.071	0.066
06:00	.000	.000	.000	.000	.062	.000	.000	.000	.067	.000	.091	.059	.024
12:00	.000	.000	.000	.000	.000	.100	.000	.000	.000	.000	.286	.077	.033
18:00	.062	.000	.040	.000	.000	.000	.057	.038	.214	.000	.000	.000	.042

TABLE VII.- PATTERN A3

G.m.t.	Months												Yearly average
	Jan.	Feb.	Mar.	Apr.	May	June	July	Aug.	Sept.	Oct.	Nov.	Dec.	
						Probability of occurrence							
00:00	0.074	0.094	0.106	0.133	0.143	0.205	0.240	0.129	0.019	0.018	0.010	0.037	0.101
06:00	.055	.106	.097	.133	.129	.186	.184	.120	.029	.023	.023	.051	.094
12:00	.074	.077	.106	.129	.115	.157	.148	.101	.024	.018	.032	.037	.085
18:00	.101	.071	.106	.119	.083	.176	.180	.124	.024	.014	.010	.060	.089
						Probability of onshore/alongshore cloud transport							
00:00	0.062	0.062	0.087	0.071	0.161	0.093	0.154	0.107	0.000	0.000	1.000	0.000	0.110
06:00	.000	.111	.048	.036	.071	.051	.100	.077	.167	.000	.200	.273	.080
12:00	.000	.000	.044	.037	.040	.000	.125	.000	.000	.250	.143	.125	.046
18:00	.046	.000	.087	.080	.056	.051	.103	.074	.000	.000	.500	.077	.071
						Probability of precipitation and onshore/alongshore cloud transport							
00:00	0.000	0.000	0.000	0.000	0.000	0.250	0.000	0.333	0.000	0.000	0.000	0.000	0.071
06:00	.000	.000	.000	.000	.000	.000	.000	.000	.000	.000	.000	.000	.000
12:00	.000	.000	.000	.000	.000	.000	.250	.000	.000	.000	.000	.000	.100
18:00	.000	.000	.000	.000	.000	.000	.000	.000	.000	.000	.000	.000	.000

TABLE VIII.- PATTERN D1

G.m.t.	Months												Yearly average
	Jan.	Feb.	Mar.	Apr.	May	June	July	Aug.	Sept.	Oct.	Nov.	Dec.	
						Probability of occurrence							
00:00	0.092	0.135	0.143	0.124	0.101	0.100	0.023	0.042	0.062	0.083	0.162	0.180	0.103
06:00	.101	.135	.152	.119	.078	.076	.074	.028	.071	.060	.133	.120	.090
12:00	.097	.129	.124	.114	.083	.110	.028	.023	.062	.078	.100	.111	.088
18:00	.124	.135	.148	.138	.097	.086	.032	.028	.052	.092	.152	.134	.101
						Probability of onshore/alongshore cloud transport							
00:00	0.150	0.000	0.032	0.038	0.091	0.190	0.400	0.111	0.077	0.333	0.118	0.051	0.103
06:00	.091	.000	.030	.040	.059	.125	.667	.333	.067	.308	.071	.000	.079
12:00	.000	.046	.037	.000	.000	.044	.167	.200	.154	.059	.174	.042	.058
18:00	.037	.044	.000	.034	.048	.000	.143	.000	.091	.150	.094	.034	.051
						Probability of precipitation and onshore/alongshore cloud transport							
00:00	0.000	0.000	0.000	1.000	0.500	0.750	0.500	0.000	0.000	0.167	0.000	0.000	0.259
06:00	.000	.000	.000	1.000	.000	.500	.000	.000	.000	.000	.000	.000	.111
12:00	.000	.000	.000	.000	.000	.000	.000	.000	.000	.000	.000	.000	.000
18:00	.000	.000	.000	.000	.000	.000	.000	.000	.000	.000	.000	.000	.000

TABLE IX.- PATTERN D2

G.m.t.	Months												Yearly average
	Jan.	Feb.	Mar.	Apr.	May	June	July	Aug.	Sept.	Oct.	Nov.	Dec.	
						Probability of occurrence							
00:00	0.152	0.200	0.138	0.071	0.046	0.014	0.005	0.014	0.033	0.042	0.100	0.074	0.072
06:00	.120	.165	.134	.066	.055	.014	.014	.005	.019	.064	.114	.115	.072
12:00	.138	.177	.120	.086	.064	.024	.018	.005	.029	.055	.152	.157	.084
18:00	.124	.171	.111	.081	.064	.029	.009	.005	.033	.055	.129	.134	.077
						Probability of onshore/alongshore cloud transport							
00:00	0.061	0.088	0.033	0.133	0.200	0.333	0.000	0.667	0.571	0.333	0.143	0.188	0.143
06:00	.115	.071	.034	.071	.083	.333	.333	1.000	.500	.286	.042	.200	.126
12:00	.167	.100	.000	.000	.143	.200	.500	.000	.167	.167	.156	.177	.127
18:00	.074	.000	.042	.000	.071	.167	.500	.000	.143	.083	.185	.069	.082
						Probability of precipitation and onshore/alongshore cloud transport							
00:00	0.000	0.000	0.000	0.000	0.000	0.000	0.000	0.500	0.000	0.000	0.000	0.000	0.038
06:00	.000	.500	.000	.000	.000	.000	1.000	.000	.500	.250	.000	.000	.174
12:00	.000	.000	.000	.000	.000	.000	.500	.000	.000	1.000	.000	.167	.148
18:00	.000	.000	.000	.000	1.000	1.000	1.000	.000	.000	.000	.000	.000	.188

TABLE X.- PATTERN B

G.m.t.	Months												Yearly average
	Jan.	Feb.	Mar.	Apr.	May	June	July	Aug.	Sept.	Oct.	Nov.	Dec.	
						Probability of occurrence							
00:00	0.217	0.153	0.101	0.110	0.111	0.029	0.028	0.032	0.171	0.327	0.267	0.184	0.143
06:00	.212	.135	.106	.119	.111	.029	.023	.042	.214	.332	.262	.170	.146
12:00	.175	.159	.111	.138	.129	.052	.037	.088	.252	.341	.257	.161	.158
18:00	.221	.159	.088	.114	.143	.048	.042	.083	.219	.327	.271	.180	.158
						Probability of onshore/alongshore cloud transport							
00:00	0.830	0.885	0.864	0.826	0.875	0.667	0.833	1.000	0.806	0.944	0.875	0.750	0.862
06:00	.739	.913	.826	.800	.833	.833	1.000	.889	.844	.958	.873	.703	.846
12:00	.868	.889	1.000	.931	.929	.727	.875	.842	.830	.946	.907	.971	.900
18:00	.729	.852	.947	.833	.774	.700	.889	.833	.898	.930	.895	.769	.857
						Probability of precipitation and onshore/alongshore cloud transport							
00:00	0.026	0.044	0.000	0.053	0.048	0.250	0.000	0.143	0.276	0.134	0.082	0.033	0.090
06:00	.059	.048	.000	.000	.100	.200	.200	.000	.132	.174	.062	.038	.090
12:00	.030	.125	.000	.037	.000	.000	.000	.000	.204	.157	.082	.000	.081
18:00	.057	.087	.056	.000	.042	.143	.125	.000	.111	.242	.078	.000	.097

TABLE XI.- PATTERN GH

G.m.t.	Months												Yearly average
	Jan.	Feb.	Mar.	Apr.	May	June	July	Aug.	Sept.	Oct.	Nov.	Dec.	
						Probability of occurrence							
00:00	0.078	0.135	0.129	0.100	0.060	0.019	0.005	0.028	0.019	0.074	0.114	0.138	0.074
06:00	.106	.188	.124	.086	.051	.014	.005	.009	.014	.088	.119	.143	.077
12:00	.106	.182	.143	.081	.069	.033	.009	.014	.010	.074	.119	.138	.080
18:00	.097	.194	.148	.086	.064	.048	.009	.037	.010	.069	.138	.138	.085
						Probability of onshore/alongshore cloud transport							
00:00	0.235	0.174	0.071	0.333	0.385	0.500	1.000	0.167	0.750	0.500	0.208	0.133	0.246
06:00	.174	.188	.148	.167	.182	.667	1.000	.500	.667	.526	.200	.032	.210
12:00	.217	.097	.161	.118	.200	.143	1.000	.333	.000	.500	.160	.133	.188
18:00	.190	.061	.094	.222	.357	.200	1.000	.250	.500	.600	.138	.167	.201
						Probability of precipitation and onshore/alongshore cloud transport							
00:00	0.000	0.000	0.000	0.000	0.200	0.000	0.000	0.000	0.000	0.125	0.000	0.000	0.044
06:00	.000	.000	.000	.000	.000	.000	.000	.000	.000	.100	.000	.000	.024
12:00	.000	.000	.000	.000	.000	.000	.000	.000	.000	.000	.000	.000	.000
18:00	.000	.000	.000	.000	.000	.000	.000	.000	.000	.000	.000	.000	.000

TABLE XII.- PATTERN E

G.m.t.	Months												Yearly average
	Jan.	Feb.	Mar.	Apr.	May	June	July	Aug.	Sept.	Oct.	Nov.	Dec.	
						Probability of occurrence							
00:00	0.028	0.029	0.032	0.010	0.032	0.067	0.028	0.046	0.038	0.060	0.005	0.018	0.033
06:00	.042	.035	.028	.010	.027	.057	.028	.060	.033	.055	.029	.018	.035
12:00	.046	.029	.046	.019	.032	.048	.032	.069	.052	.046	.052	.023	.042
18:00	.028	.035	.037	.024	.042	.052	.028	.060	.043	.051	.024	.023	.037
						Probability of onshore/alongshore cloud transport							
00:00	0.167	0.400	0.429	0.000	0.286	0.643	0.500	0.700	0.500	0.615	1.000	0.750	0.518
06:00	.333	.333	.500	.000	.167	.667	.667	.539	.429	.667	.667	.750	.517
12:00	.300	.200	.200	.250	.429	.600	.429	.333	.727	.600	.182	.000	.384
18:00	.500	.333	.250	.000	.444	.546	.333	.538	.667	.727	.200	.200	.447
						Probability of precipitation and onshore/alongshore cloud transport							
00:00	1.000	0.000	0.333	0.000	0.333	0.444	0.333	0.143	0.750	0.375	1.000	0.333	0.383
06:00	.667	.500	.667	.000	.000	.500	.500	.143	.000	.125	.500	.333	.314
12:00	.667	.000	.000	1.000	.000	.833	.000	.000	.250	.167	.000	.000	.250
18:00	.333	.000	.000	.000	.250	.667	.000	.000	.167	.250	.000	.000	.217

TABLE XIII.- PATTERN LV

G.m.t.	Months												Yearly average
	Jan.	Feb.	Mar.	Apr.	May	June	July	Aug.	Sept.	Oct.	Nov.	Dec.	
						Probability of occurrence							
00:00	0.078	0.082	0.055	0.110	0.120	0.171	0.184	0.152	0.129	0.069	0.081	0.092	0.111
06:00	.092	.071	.046	.119	.124	.200	.244	.207	.138	.074	.100	.088	.126
12:00	.083	.082	.042	.133	.111	.162	.212	.203	.129	.083	.076	.069	.116
18:00	.064	.065	.042	.119	.115	.152	.221	.152	.119	.078	.062	.051	.104
						Probability of onshore/alongshore cloud transport							
00:00	0.294	0.074	0.417	0.391	0.500	0.611	0.550	0.576	0.593	0.667	0.235	0.350	0.475
06:00	.350	.250	.500	.480	.333	.643	.528	.600	.414	.562	.143	.421	.470
12:00	.222	.214	.778	.357	.417	.382	.391	.568	.482	.389	.188	.400	.406
18:00	.500	.182	.444	.400	.400	.469	.417	.636	.560	.471	.462	.273	.456
						Probability of precipitation and onshore/alongshore cloud transport							
00:00	0.000	0.000	0.000	0.000	0.000	0.136	0.182	0.105	0.000	1.000	0.000	0.000	0.075
06:00	.000	.000	.000	.083	.000	.037	.036	.111	.000	.000	.000	.000	.040
12:00	.000	.000	.000	.000	.000	.077	.000	.000	.000	.000	.000	.000	.008
18:00	.000	.000	.000	.000	.000	.067	.000	.048	.000	.000	.000	.000	.017

REFERENCES

1. Dumbauld, R. K.; and Bjorklund, J. R.: NASA/MSFC Multilayer Diffusion Models and Computer Programs, Version 5. NASA CR-2631, 1975.

2. Gregory, Gerald L.; and Storey, Richard W., Jr.: Effluent Sampling of Titan III C Vehicle Exhaust. NASA TM X-3228, 1975.

3. Stewart, Roger B.; Sentell, Ronald J.; and Gregory, Gerald L.: Experimental Measurements of the Ground Cloud Effluents and Cloud Growth During the February 11, 1974, Titan-Centaur Launch at Kennedy Space Center. NASA TM X-72820, 1976.

4. Bendura, Richard J.; and Crumbly, Kenneth H.: Ground Cloud Effluent Measurements During the May 30, 1974, Titan III Launch at the Air Force Eastern Test Range. NASA TM X-3539, 1977.

5. American Meteorological Society, 1977 Committee on Atmospheric Turbulence and Diffusion: Accuracy of Dispersion Models. Bull. American Meteorol. Soc., vol. 59, no. 8, Aug. 1978, pp. 1025-1026.

1. Report No.	2. Government Accession No.	3. Recipient's Catalog No.
NASA TM-58224		

4. Title and Subtitle	5. Report Date
A DIFFUSION CLIMATOLOGY FOR CAPE CANAVERAL, FLORIDA	April 1980
	6. Performing Organization Code: JSC-16496
7. Author(s): Richard K. Siler	8. Performing Organization Report No.
9. Performing Organization Name and Address: Lyndon B. Johnson Space Center, Houston, Texas 77058	10. Work Unit No.: 152-85-00-00-72
	11. Contract or Grant No.
12. Sponsoring Agency Name and Address: National Aeronautics and Space Administration, Washington, D.C. 20546	13. Type of Report and Period Covered: Technical Memorandum
	14. Sponsoring Agency Code

15. Supplementary Notes

16. Abstract

The problem of toxic effluent released by a Space Shuttle launch on local plant and animal life is discussed. Based on several successive years of data, nine basic weather patterns are identified, and the probabilities of pattern occurrence, of onshore/alongshore cloud transport, of precipitation accompanying the latter, and of ground-level concentrations of hydrogen chloride are determined. Diurnal variations for the patterns are also investigated. Sketches showing probable movement of launch-cloud exhaust and isobaric maps are included.

17. Key Words (Suggested by Author(s))

Space Shuttle
Exhaust cloud
Launch effluent
Launch scheduling
Diffusion climatology
Diffusion model

18. Distribution Statement

STAR Subject Category:
47 (Meteorology and Climatology)

19. Security Classif. (of this report)	20. Security Classif. (of this page)	21. No. of Pages	22. Price*
Unclassified	Unclassified	49	$4.00

*For sale by the National Technical Information Service, Springfield, Virginia 22161

☆ U.S. GOVERNMENT PRINTING OFFICE: 1980 — 671-099/1612

NASA — JSC